Nanotechnology

DOI: 10.1002/anie.200600394

Surface Plasmon Resonances of Free-Standing Gold Nanowires Fabricated by Nanoskiving**

*Qiaobing Xu, Jiming Bao, Federico Capasso, and George M. Whitesides**

Herein we present both a simple, experimentally convenient method for the fabrication of gold nanowires with uniform, controlled dimensions (Figure 1), and a systematic study of the dependence of the plasmon resonance of these gold nanowires on the geometry of these wires. The length of the wires is determined by photolithography; the width is determined by the thickness of a film fabricated by deposition from the vapor; the height is determined by sectioning ("nanoskiving") with the diamond knife of a microtome.[1,2] The cross sections of the wires can be as small as 10 nm × 30 nm. We measure the surface plasmon resonances of individual gold wires, and show these resonances to be determined by their cross-sectional dimensions.

Nanoparticles of noble metals (Ag or Au) show different colors as a result of their surface plasmon resonances.[3,4] These particles interact strongly with visible light through the resonant excitation of the collective oscillations of their conduction electrons.[3,4] As a result of these oscillations, local

[*] Q. Xu, Prof. G. M. Whitesides
Department of Chemistry and Chemical Biology
Harvard University
Cambridge, MA 02138 (USA)
Fax: (+1) 617-495-9857
E-mail: gwhitesides@gmwgroup.harvard.edu
Dr. J. Bao, Prof. F. Capasso
Division of Engineering and Applied Sciences
Harvard University
Cambridge, MA 02138 (USA)

[**] This research was supported by the NIH (GM065364), by DARPA (sub-award to G.M.W. from the Center for Optofluidic Integration at the California Institute of Technology), and by a MURI AFOSR sub-award to F.C. MRSEC and NSEC shared facilities supported by the NSF under awards DMR-0213805 (MRSEC) and PHY-0117795 (NSEC) were utilized. We thank Ertugrul Cubukcu, Dr. Marko Loncar, Dr. Brian Mayers, and Prof. Kenneth Crozier for helpful discussions.

Supporting information for this article is available on the WWW under http://www.angewandte.org or from the author.

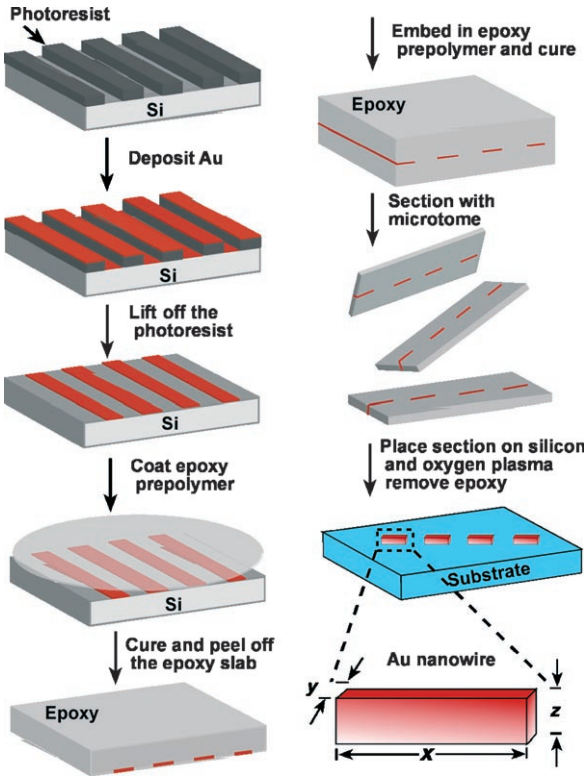

Figure 1. Schematic illustration of the procedure used to fabricate metal nanowires with a controllable size. The length of the metal structure (*x*) is determined by photolithography (ca. 2 μm), and the width of the structures (*y*) is determined by the thickness of the deposited metal film (10, 20, or 40 nm). The thickness of the sectioned polymer slab (*z*) is controlled by the microtome (30, 50, 70, or 100 nm).

electromagnetic fields near the particle can be many orders of magnitude higher than the incident fields; these strong, oscillating fields generate intense scattered light around the wavelength of the resonant peak. The magnitude, peak wavelength, and spectral bandwidth of the plasmon resonance of a nanoparticle depend on the size, shape, material of fabrication, and local environment of the particle.[3–6] The enhancement in local field and strong scattering is useful for a number of applications, including surface-enhanced Raman scattering,[7,8] subwavelength optical waveguides,[9–16] biolabels,[17–19] and biosensors.[20–25]

Nanostructures with different geometries in a range of materials have been synthesized by using chemical methods.[26–32] These nanostructures are usually not uniform in size nor geometry. The integration of these nanostructures into optical devices is also challenging because of the difficulty of selecting and manipulating specific nanoparticles. Nanoparticles fabricated by nanosphere lithography have been used for chemosensing and biosensing.[21–24] This technique, although very useful, can only produce nanostructures with limited flexibility in dimensions and geometries. Electron-beam lithography is widely used to fabricate metal nanostructures for studying surface plasmon coupling and subwavelength optical waveguides.[9,13–16,33–35] However, electron-beam lithography is still not conveniently available to general users, and it is also challenging to fabricate wires with widths below 30 nm and high aspect ratios. Exploration and development of new techniques for the fabrication of nanostructures relevant to plasmonics is desirable.[36,37] The technique described herein is not intended to replace these existing methods, but rather to provide a simple alternative for the fabrication of relevant nanostructures with well-controlled dimensions, and to aid the study of their optical properties.

Figure 1 shows the procedure used to fabricate free-standing gold nanowires. This procedure combines photolithography, vapor deposition, and microtome sectioning; we have used a related procedure previously to fabricate nanoelectrodes.[1] We first generated a pattern with rectangular lines (2-μm wide with 2-μm spacing in this case) on a silicon substrate (with 2-nm-thick native oxide) by using standard photolithography with a Shipley 1805 photoresist. We subsequently deposited 10–40 nm of gold film by using electron-beam evaporation on this patterned substrate. Removal of the photoresist with acetone generated gold wires (10–40-nm thick and 2-μm wide) on the silicon substrate. We then cast a layer of epoxy (araldite 502) prepolymer on this substrate. After curing the epoxy, we mechanically peeled it from the substrate; the gold film transferred to the epoxy film because of the weak adhesion between the gold and the silicon substrate. We embedded this epoxy substrate into more of the epoxy prepolymer; curing generated an epoxy slab containing a layer of embedded, patterned metal film.

We sectioned the epoxy block in a plane that intersected the wire perpendicularly by using a microtome (Leica MZ6) equipped with a diamond knife (Diatome ultra 35°) and with water filling the sample-collection boat.[2] Sectioning with a microtome generated polymer slabs with thickness ranging from 30 to 100 nm; these slabs floated at the air–water interface in the sample-collection boat. We transferred the epoxy sections to a bare silicon substrate by immersing it in the water, and withdrawing it in a way that the floating polymer films were captured by means of capillarity. Before optical characterization of the gold nanowires, we removed the polymer matrix by using an oxygen plasma; this process left the gold nanowires intact and supported on the silicon substrate, usually in the orientation in which they were embedded in the slab. The length (*x*) of the nanowires is defined by the width of the initial wires relative to the plane of the sections (2 μm for all the samples described herein, but this length can be longer or much shorter). Figure 2 shows the SEM image of gold nanowires with two different sizes. These free-standing wires usually do not fall over even when they have a large height-to-width ratio; we attribute this stability in orientation to the interfacial interaction between the gold and the silicon dioxide of the substrate.

Standard light microscopes equipped with dark-field illumination have been used extensively to study the surface plasmon behavior of nanostructures.[3,4,17] Figure 3a outlines the apparatus used to select individual nanowires and record their scattering spectrum. We illuminated the nanowires with unpolarized, focused, white light from a high-intensity fiber light source (Fiber Illuminator OSL1). The incident beam of light was perpendicular to the long axis of the nanowire at an angle of about 60° with respect to the normal of the silicon

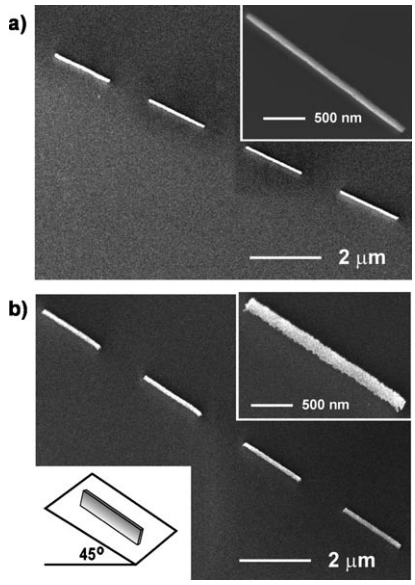

Figure 2. SEM images of typical free-standing gold nanowires viewed on an angle. a) Gold nanowires with dimensions (x, y, z) of approximately 2 μm × 40 nm × 50 nm. b) Gold nanowires with dimensions of approximately 2 μm × 10 nm × 100 nm. The insets show high-magnification images of the same samples. The orientations of (a) and (b) are at a 45° oblique angle.

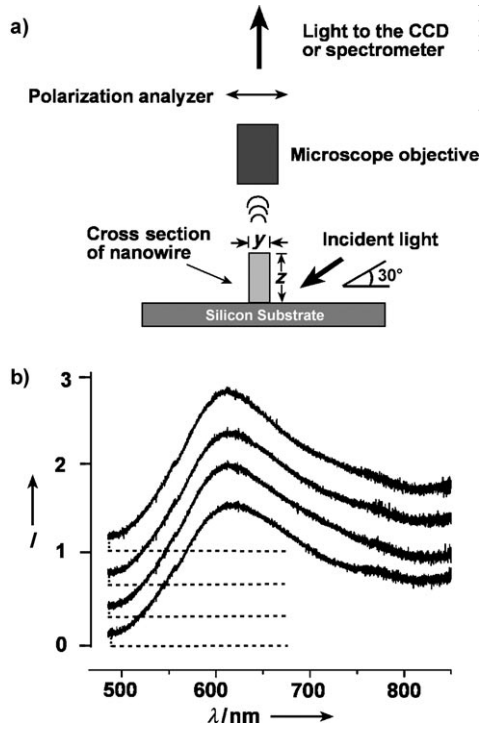

Figure 3. a) Experimental setup used for measurement of optical scattering of gold nanowires. b) The scattering spectra of four randomly selected individual nanowires (2 μm × 20 nm × 50 nm). The spectra are vertically displaced to show reproducibility.

substrate. Scattered light from the nanowire was collected selectively through a microscopic objective with a long working distance (Mitutoyo SL50, numerical aperture (NA) = 0.55). This dark-field illumination maximized the scattering from the nanoparticles, and minimized the background scattering from the substrate. The collected light then passed through a polarizer parallel to the short axis of the nanowire (y direction) and focused on the plane of the entrance slit of a single-grating monograph (Jobin Yvon Horiba Triax 550); this apparatus allowed us both to take a video image of the nanowires and to measure their spectrum. The polarizer allowed us to select surface plasmon resonances with polarization traverse to the long axis of the wire. An individual nanowire, or a small group of nanowires, could be selected for analysis by adjusting the width and height of the slit. The spectra obtained depended on the spectrum of the incident white light, the focusing and collecting optics, and the response of the spectrometer. To remove these effects and isolate the plasmon resonance spectrum of the nanowires, we replaced the nanowire sample with a broad-band white-light target (which has a constant scattering response over wide range of frequencies) and obtained its scattering spectrum by using the same procedure. We then normalized the obtained spectrum of the nanowires to the reference spectrum of the broad-band target.[17] Figure 3b shows the normalized scattering spectra of four nanowires randomly selected from a single sample. The variation in position of the resonance peak among the nanowires is negligible. We also found the spectral variation between nanowires from separate slabs of the same thickness to be negligible. These observations established the optical homogeneity of the nanowires generated by this sectioning technique, and implied their constancy in size.

We fabricated nanowires with different cross-sectional dimensions by changing the thicknesses of the metal film and the sections. Figure 4a–c shows color, dark-field, optical images of nanowires with different cross sections obtained by using a standard optical microscopic with dark-field illumination (Nikon 43300–522 with CCD camera). All optical images were obtained under the same conditions with polarization perpendicular to the long axis of the nanowires. For each set of wires with the same width (y), the color shows a red shift with increasing nanowire height (z). Figure 4d–f shows the scattering spectra of the gold nanowires shown in Figure 4a–c. We usually collected the emission from four nanowires simultaneously to increase the signal-to-noise ratio and to average the small spectral variations betweens the wires. The peak maximum shifts to longer wavelength with increase in the height of wires from the same set with fixed width. This observation agrees well with the optical color images.

To rationalize these spectra, we simulated them by using finite-difference time-domain (FDTD) techniques.[38] The frequency-dependent dielectric constant of gold was obtained from the literature.[39] The configuration of the simulation was the same as that in the experiment (Figure 3a) except that in the simulation the wire was suspended in air rather than supported on the Si/SiO_2 substrate. For each simulation, the plane of the incident excitation wave was at the same angle (60°). We calculated the scattering amplitude at individual wavelengths and obtained the far-field scattered field. The scattering spectrum was then calculated by integrating the scattered field over angles set by the numerical aperture of the collecting objective (NA = 0.55). Figure 5a–c shows the

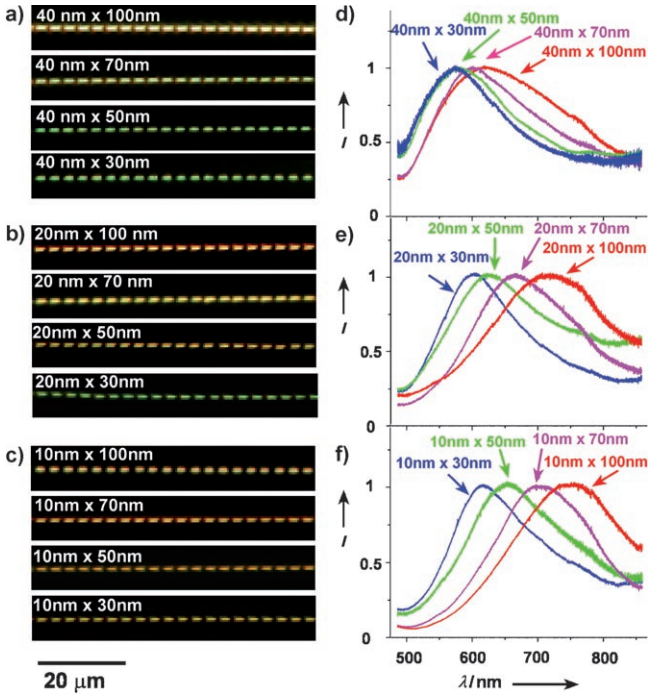

Figure 4. Surface plasmon resonances of gold nanowires with different cross-sectional dimensions. a–c) Dark-field optical images of gold nanowires having different dimensions (all 2-μm long (*x*); dimensions of the cross section marked in the figure as *y*×*z*). The nanowires appear larger than their actual dimensions owing to optical diffraction. d–f) Scattering spectra of gold nanowires with different dimensions, corresponding to the gold nanowires shown in (a–c).

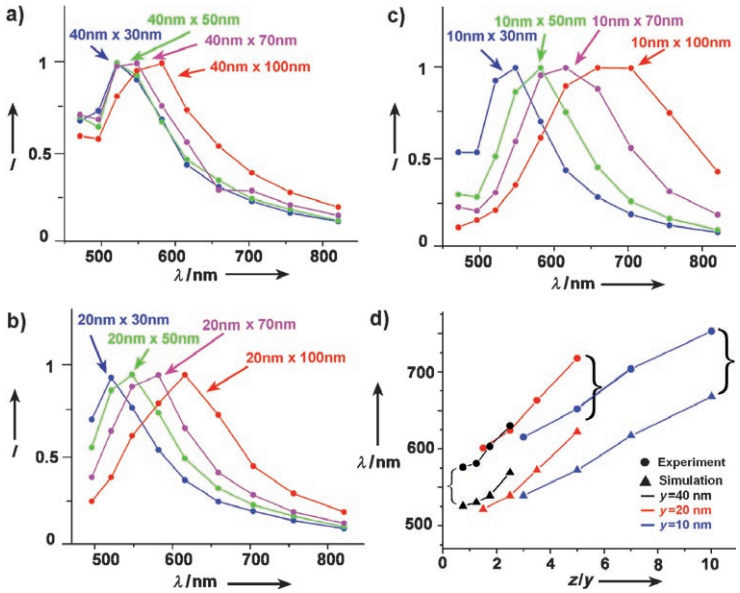

Figure 5. FDTD simulations and comparison with experimental results. a–c) Finite-difference time-domain simulations of scattering spectra. For each set of fixed widths (10, 20, or 40 nm), the resonance peak moves to longer wavelength as the height increases. The dimensions of the cross section are marked in each figure as *y*×*z*. d) Dependence of maximum wavelength of the scattering resonances as a function of aspect ratio *z*/*y* for data from experiment and FDTD simulation. The corresponding experimental and simulation data are paired by braces for clarity.

results of these FDTD simulations. The simulations and the experimental results showed the same trend in the red shift of the maxima as the *z*/*y* ratio increased. Since the polarization of the incident light was at 60° with respect to the *z* axis in the *z*–*y* plane, two modes of surface plasmons, polarized along the *z* and *y* directions, were excited. The total scattering spectrum arises from the plasmons excited by the *z* and *y* components of the incident electric field. Analysis of data from the simulations shows that the scattered field was almost the superposition of fields generated by two dipoles oscillating along the *z* and *y* directions. In our experimental configuration, the light-collection efficiency for *y*-polarized emission is 8 times larger than for *z*-polarized emission, and the contributions to the recorded intensity are about equal when the *z*/*y* aspect ratio is 1.5. For wires with aspect ratios larger than 1.5, the spectra are dominated by the scattering generated by *z*-polarized plasmons, especially near the resonance wavelength. Figure 5 d plots the dependence of the wavelength of maximum plasmon scattering on the *z*/*y* aspect ratio (from 0.75 to 10) for the experimental measurements and the simulation. Both the experimental data and the FDTD simulation showed a similar red shift when the aspect ratio of the nanowire cross section increased. The resonance peaks of the experimental data were, however, consistently at longer wavelengths than those of the simulations (Figure 5 d). We believe that this discrepancy reflects the fact that the simulations assumed that the nanowires were suspended in air rather than supported on silicon substrates with a thin layer of native SiO_2. Similar effects have been reported.[14,15]

The technique we describe herein offers a convenient way to make free-standing gold nanostructures with uniform and well-controlled size and shape. These structures are well-suited for fundamental studies of the relationships between the shape of nanostructures and their properties as plasmon resonators. This technique can be used to fabricate nanostructures that are impossible or very difficult to make with other techniques. It can be used with most metals that can be deposited from the vapor (we are still investigating the behavior of brittle materials upon sectioning). A major benefit of this technique is that the nanostructures can be easily positioned by manipulating the macroscopic epoxy slabs (the epoxy can be removed conveniently after positioning by oxygen plasma etching). The ability to tune the shape and composition of the nanostructures, and the ability to position the nanostructures, will, we believe, combine to make this technique useful in the fabrication of prototype optical devices such as subwavelength optical waveguides and biosensors.

Received: January 30, 2006
Published online: April 28, 2006

Keywords: gold · microtome · nanotechnology · sectioning · surface plasmon resonance

[1] Q. Xu, B. D. Gates, G. M. Whitesides, *J. Am. Chem. Soc.* **2004**, *126*, 1332.

[2] A. M. Glauert, *Practical Methods in Electron Microscopy*, Elsevier, New York, **1974**.
[3] C. F. Bohren, D. R. Huffman, *Absorption and Scattering of Light by Small Particles*, Wiley, New York, **1983**.
[4] U. Kreibig, M. Vollmer, *Optical Properties of Metal Clusters*, *Vol. 25*, Springer, Berlin, **1995**.
[5] S. Link, M. A. El-Sayed, *J. Phys. Chem. B* **1999**, *103*, 8410.
[6] K. L. Kelly, E. Coronado, L. L. Zhao, G. C. Schatz, *J. Phys. Chem. B* **2003**, *107*, 668.
[7] X. S. Xie, *Acc. Chem. Res.* **1996**, *29*, 598.
[8] S. Nie, S. R. Emory, *Science* **1997**, *275*, 1102.
[9] J.-C. Weeber, A. Dereux, C. Girard, J. R. Krenn, J.-P. Goudonnet, *Phys. Rev. B* **1999**, *60*, 9061.
[10] W. L. Barnes, A. Dereux, T. W. Ebbesen, *Nature* **2003**, *424*, 824.
[11] K. B. Crozier, A. Sundaramurthy, G. S. Kino, C. F. Quate, *J. Appl. Phys.* **2003**, *94*, 4632.
[12] P. G. Kik, S. A. Maier, H. A. Atwater, *Mater. Res. Soc. Symp. Proc.* **2002**, *705*, 101.
[13] S. A. Maier, H. A. Atwater, *J. Appl. Phys.* **2005**, *98*, 011101.
[14] G. Schider, J. R. Krenn, W. Gotschy, B. Lamprecht, H. Ditlbacher, A. Leitner, F. R. Aussenegg, *J. Appl. Phys.* **2001**, *90*, 3825.
[15] J. R. Krenn, B. Lamprecht, H. Ditlbacher, G. Schider, M. Salerno, A. Leitner, F. R. Aussenegg, *Europhys. Lett.* **2002**, *60*, 663.
[16] D. A. Genov, V. M. Shalaev, A. K. Sarychev, *Phys. Rev. B* **2005**, *72*, 113102.
[17] S. Schultz, D. R. Smith, J. J. Mock, D. A. Schultz, *Proc. Natl. Acad. Sci. USA* **2000**, *97*, 996.
[18] D. A. Schultz, *Curr. Opin. Biotechnol.* **2003**, *14*, 13.
[19] C. Loo, L. Hirsch, M.-H. Lee, E. Chang, J. West, N. Halas, R. Drezek, *Opt. Lett.* **2005**, *30*, 1012.
[20] Y. C. Cao, R. Jin, C. A. Mirkin, *Science* **2002**, *297*, 1536.
[21] A. J. Haes, R. P. Van Duyne, *J. Am. Chem. Soc.* **2002**, *124*, 10596.
[22] A. J. Haes, L. Chang, W. L. Klein, R. P. Van Duyne, *J. Am. Chem. Soc.* **2005**, *127*, 2264.
[23] A. J. Haes, S. Zou, G. C. Schatz, R. P. Van Duyne, *J. Phys. Chem. B* **2004**, *108*, 109.
[24] C. R. Yonzon, E. Jeoung, S. Zou, G. C. Schatz, M. Mrksich, R. P. Van Duyne, *J. Am. Chem. Soc.* **2004**, *126*, 12669.
[25] L. R. Hirsch, J. B. Jackson, A. Lee, N. J. Halas, J. L. West, *Anal. Chem.* **2003**, *75*, 2377.
[26] Y. Xia, N. J. Halas, *MRS Bull.* **2005**, *30*, 338.
[27] M. A. El-Sayed, *Acc. Chem. Res.* **2001**, *34*, 257.
[28] R. Jin, Y. Cao, C. A. Mirkin, K. L. Kelly, G. C. Schatz, J. G. Zheng, *Science* **2001**, *294*, 1901.
[29] J. J. Mock, S. J. Oldenburg, D. R. Smith, D. A. Schultz, S. Schultz, *Nano Lett.* **2002**, *2*, 465.
[30] Y. Xiong, J. Chen, B. Wiley, Y. Xia, Y. Yin, Z.-Y. Li, *Nano Lett.* **2005**, *5*, 1237.
[31] C. L. Nehl, N. K. Grady, G. P. Goodrich, F. Tam, N. J. Halas, J. H. Hafner, *Nano Lett.* **2004**, *4*, 2355.
[32] B. Wiley, Y. Sun, J. Chen, H. Cang, Z.-Y. Li, X. Li, Y. Xia, *MRS Bull.* **2005**, *30*, 356.
[33] S. A. Maier, P. G. Kik, H. A. Atwater, S. Meltzer, E. Harel, B. E. Koel, A. A. G. Requicha, *Nat. Mater.* **2003**, *2*, 229.
[34] K. H. Su, Q. H. Wei, X. Zhang, J. J. Mock, D. R. Smith, S. Schultz, *Nano Lett.* **2003**, *3*, 1087.
[35] Q. H. Wei, K. H. Su, S. Durant, X. Zhang, *Nano Lett.* **2004**, *4*, 1067.
[36] Y. Xia, G. M. Whitesides, *Angew. Chem.* **1998**, *110*, 568; *Angew. Chem. Int. Ed.* **1998**, *37*, 550.
[37] B. D. Gates, Q. Xu, M. Stewart, D. Ryan, C. G. Willson, G. M. Whitesides, *Chem. Rev.* **2005**, *105*, 1171.
[38] XFDTD, a full-wave time-domain solver from REMCOM (http://www.remcom.com).
[39] P. B. Johnson, R. W. Christy, *Phys. Rev. B* **1972**, *6*, 4370.

